

Land Surface Temperature Estimation Using Landsat 9 Satellite Imagery in Lamongan Regency, Indonesia


Alifah Noraini *

Geodetic Engineering, Institut Teknologi Nasional
Malang,
Malang, 65152, Indonesia
alifah.aini09@gmail.com

**Corresponding author*

I Nyoman Sudiasa

Civil Engineering, Institut Teknologi Nasional Malang,
Malang, 65152, Indonesia
nyomansudiasa@yahoo.co.id

 Submitted: 2023-02-22; Accepted: 2023-12-31; Published: 2024-12-06

Abstract—Gerbangkertosusila area (Gresik, Bangkalan, Mojokerto, Surabaya, Sidoarjo, and Lamongan) is a target area for accelerating economic development. Land use changes are one of the phenomena that often occur in districts that have the potential for developing the area, one of the areas that has the potential to become a Creative Economy Zone is Lamongan Regency. This study aims to estimate changes in Land Surface Temperature (LST) in Lamongan Regency by utilizing Landsat 9 satellite imagery. Landsat 9 satellite imagery is processed based on a temperature algorithm for estimating temperature calculations. The Landsat 9 satellite was launched in 2021 and is a replacement satellite for the Landsat 8 satellite. The Landsat 9 satellite has 9 spectral bands and 2 thermal bands. Estimation of LST uses band 4, band 5, and band 10. The LST algorithm used is the mono window algorithm. The mosaic process was carried out on path 118 raw 65 and path 119 raw 65. The results showed that the Lamongan Regency area has a greenish level with a value range of (-0.611) to 0.5 which is dominated by medium density levels. The estimation results of LST in Lamongan Regency are dominated by temperatures in the range of 23°C – 26°C with the highest temperature being 29°C – 33°C.

Keywords— Estimation, Landsat 9 Satellite Imagery, LST, Mono window algorithm, Temperature

I. INTRODUCTION

Gerbangkertosusila area (Gresik, Bangkalan, Mojokerto, Surabaya, Sidoarjo, and Lamongan) is a target area for accelerating economic development according to Presidential Decree 80 of 2019 (Gunawan, 2021). According to the Head of the East Java One-Stop Investment and Services Agency/ *Dinas Penanaman Modal dan Pelayanan Terpadu Satu Pintu* (PMPTSP), Lamongan Regency is included in the priority area. So that Lamongan Regency needs to have a minimum of 50

hectares of Industrial Area (Kementrian Perindustrian Republik Indonesia, 2021). The Provincial Government of East Java has designated the northern area of Lamongan Regency on 2022, especially Brondong District, as a Special Economic Zone/ *Kawasan Ekonomi Khusus* (KEK) for the maritime industry sector which will soon be developed with an area of 200 hectares of land provided. The rise of industrial development in Lamongan Regency has resulted in significant land conversion. Agricultural land cover will be converted into buildings. This will affect the temperature in Lamongan Regency. From this background, research will be carried out on land surface temperature to determine changes in temperature in Lamongan Regency temporally.

This research utilizes remote sensing to estimate Land Surface Temperature (LST). Remote sensing is "A science and art of obtaining information about objects, areas or phenomena through the analysis of data obtained using tools without direct contact with the objects, areas or phenomena being studied" (Lillesand, Kieffer, & Chipman, 2004). The sensory system consists of various components that are integrated into one unit. These components include sources of energy, atmosphere, objects, sensors with vehicles, data processing, interpretation or analysis and users.

Land Surface Temperature (LST) can be described as the temperature of the earth's surface and it most important parameters in climate change, evapotranspiration, urban climate, vegetation monitoring, and environmental studies. LST calculated from remote sensing data, is used in many areas of science such as hydrology, forestry, agriculture, etc. (Guillevic, et al., 2018). LST is one important indicator to understand the spatial change and surface processes on the earth surface that leads to actual assessment of environmental quality. The relation between spatial analysis of LST and existing Land Use/ Land Cover (LULC) changes is important to evaluate climate processes (Ibrahim & Mallouh, 2018). The satellite imagery used in this study is Landsat 9 satellite imagery.

Many LST retrieval algorithms based on remotely sensed images have been introduced, where the Land

Surface Emissivity (LSE) is one of the main factors affects the accuracy of the LST estimation. The algorithm can be estimated of LST such as Mono Window Algorithm (MWA), Radiative Transfer Equation (RTE) method, Single Channel Algorithm (SCA) and Split Window Algorithm (SWA) (Sekertekin & Bonafoni, 2020). Three algorithm (MWA; SWA; and Sigle Channel/ SC) show that all three algorithms in term of input parameters, accuracy, and sensitivity can achieve good results in retrieving the LST. The SWA is the least sensitive to the error of the input parameters. The MWA and SC method are sensitive to the error of the input parameters, and compared with the error of the LSE, these two algorithms are more sensitive to the error of atmospheric water vapor content. The MWA is also very sensitive to the error of the effective mean atmospheric temperature (Wang, Lu, & Yao, 2019).

II. RESEARCH METHODS

The study area was on Lamongan Regency, Indonesia. Figure 1 shows, Lamongan regency is located at 6°51' - 7°23' S and 112°33' - 112°34' E with an area of ±1,812.8 km². The boundaries of the Lamongan Regency area are as follows:

1. North : Java Sea
2. East : Gresik Regency
3. South : Jombang and Mojokerto Regencies
4. West : Bojonegoro and Tuban Regencies

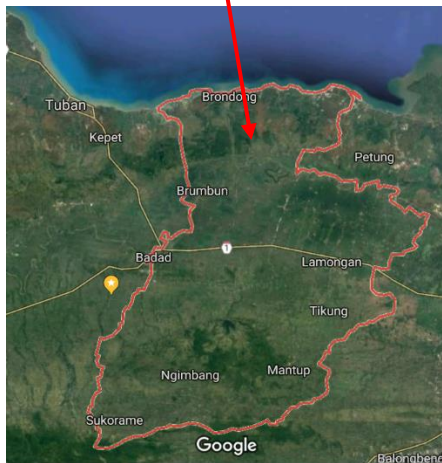


Figure. 1. Lamongan Regency, Indonesia

A Landsat 9 imagery listed in covering Lamongan, Indonesia were acquired from the United States Geological Survey Earth Explorer free online data services for LST. Landsat 9 was launched on September 27, 2021 in California by a partnership between NASA and the U.S. Geological Survey. Landsat 9 has a higher imaging capacity than past Landsat, allowing more valuable data to be added to the Landsat global and archive around 1,400 scenes per day. Landsat 9 and Landsat 8 have radiometrically and geometrically better than earlier generation Landsat (U.S.Geological Survey, <https://earthexplorer.usgs.gov/>, 2022) Landsat 9 satellite characteristics are listed in Table 1.

Table 1. Landsat 9 Characteristics

Science instruments	OLI-2; TIRS-2
OLI-2 build	Ball Aerospace & Technology Corp.
TIRS-2 build	NASA Goddard Space Flight Center
Design life	5 years
Spacecraft provider	Northrop Grumman Innovative Systems (NGIS)
Image data	>700 scenes per day
Launch data	September 27, 2021
Launch vehicle	Authors' names
Launch location	Vandenberg Space Force Base, California
Orbit	Near-polar, sun synchronous at an altitude of 438 miles (705 km)
Orbital inclination	98.2°
Spacecraft speed	16,760 mi/hr (26,972 km/hr)
Consumables	10 years
Band	Operational Land Imager 2 (OLI-2) 9 (nine) spectral band:
	1. Band 1 visible (0.43 – 0.45 μm) 30 m
	2. Band 2 visible (0.45 – 0.51 μm) 30 m
	3. Band 3 visible (0.53 – 0.59 μm) 30 m
	4. Band 4 red (0.64 – 0.67 μm) 30 m
	5. Band 5 near-infrared (0.85 – 0.88 μm) 30 m
	6. Band 6 SWIR 1 (1.57 – 1.65 μm) 30 m
	7. Band 7 SWIR 2 (2.11 – 2.29 μm) 30 m
	8. Band 8 Panchromatic (PAN) (0.50 – 0.68 μm) 30 m
	9. Band 9 Cirrus (1.36 – 1.38 μm) 30 m
	Thermal Infrared Sensor 2 (TIRS-2) 2 (two) spectral bands:
10. Band 10 TIRS 1 (10.6 – 11.9 μm) 100 m	
11. Band 11 TIRS 2 (11.5 – 12.51 μm) 100 m	

Source: (U.S.Geological Survey, Landsat 9, 2021)

To process satellite imagery, two task were used is image pre-processing and image analysis. In image processing, OLI-2 spectral band i.e. band 4 and band 5; thermal infrared band (band 10) were selected. Figure 2. shows this research using two scene satellite imagery (path 118/ raw 065 and path 119/ raw 065) and need to process mosaic.

Mosaic is process to merging two or more raster data to single data. Areas with the same spatial reference have been matched and dissolved. Figure 3 is the result of a mosaic in Lamongan Regency. Two scenes in adjacent areas are combined into one image without gaps.

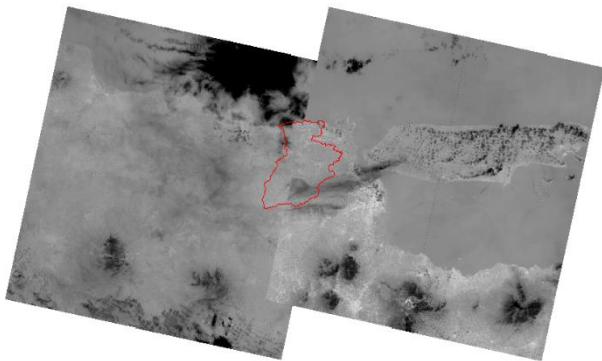


Figure. 2. Landsat 9 image covering study area with Lamongan area boundary

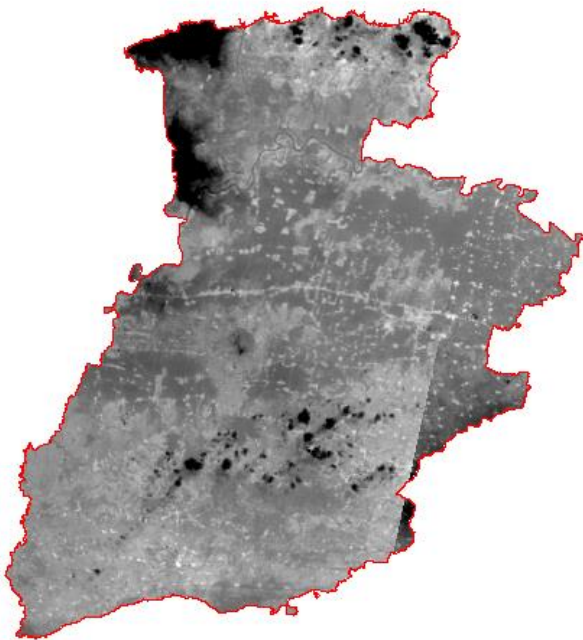


Figure. 3. Area of Interest Lamongan Regency

Lamongan Regency shapefiles (boundary line were acquired from Badan Informasi Geospasial) were used to extract from the full scenes to cropping area of interest. All the images were projected to the Universal Transverse Mercator (UTM) coordinates zone 49 south. The spheroid and datum was also to WGS 84.

LST is surface temperature measured by remote sensing sensors. LST was estimated from the Top of Atmosphere brightness value from the infrared spectral band. Estimates are affected by land cover and soil moisture (Copernicus, 2021). Based on research conducted by (Pardede, 2010) concerning the relationship between surface temperature

and land cover, it was found that land cover types with little vegetation, namely open land and settlements, had the highest surface temperatures, namely 26.99°C - 30.91°C. A bivariate correlation of -0.522 indicates an inverse relationship between surface temperature and NDVI, which means that the higher the vegetation density, the lower the surface temperature in Medan City and Deli Serdang Regency.

In the first step of LST estimation is converting Digital Number (DN) to Top of Atmosphere (TOA) radiance (Mustafa, 2020); (Sutariya, Hirapara, & Tiwari, 2022). Band 10 from Landsat 9 TIRS data has been used for estimation of top atmospheric spectral radiance. It can be calculating following (1)

$$L\lambda = M_L * Q_{cal} + A_L \tag{1}$$

$L\lambda$: TOA spectral radiance (W/Cm²*Sr* μ m)

ML : Band-specific multiplicative rescaling factor from the metadata

AL : Band-specific additive rescaling factor from the metadata

QCAL: Quantized and calibrated standard product pixel value (DN)

After the convert process is complete, the TOA spectral radiance is converted to the brightness temperature value in °C units using the equation (2)

$$BT = \left(\frac{K_2}{\ln\left(\frac{K_1}{L\lambda} + 1\right)} \right) - 273,15 \tag{2}$$

BT : Top of atmosphere brightness temperature (°C)

$L\lambda$: TOA spectral radiance (W/Cm²*Sr* μ m)

K1 : band specific thermal conversion constant from the metadata

K2 : band specific thermal conversion constant from the metadata

AL and ML values in equation 1 and also K1 and K2 values in equation 2 can be obtained from Landsat 9 satellite imagery metadata.

Table 1. K values and Rescalling factor

No	Thermal constant	Band 10
1	ML	0.0038
2	AL	0.1
3	K1	799.0284
4	K2	1329.2405

Source: (U.S.Geological Survey, Landsat 9, 2021)

Calculating Vegetation Index is part of the process of estimation LST. Vegetation index was generated from processing satellite imagery using the Normalized Difference Vegetation Index (NDVI) Landsat 9 method using band 4 (red) and band 5 (near infrared) (Celik, Kaya, Alganci, & Seker, 2019). In addition to producing vegetation index, the results of the NDVI process are used

for calculations for the LST process. NDVI method uses equation (3).

$$NDVI = \frac{(b5-b4)}{(b5+b4)} \quad (3)$$

b5: band 5 Landsat 9

b4: band 4 Landsat 9

The formula NDVI generated a value between -1 and +1. If it had low reflectance (or low values) in the red channel and high reflectance in the NIR channel (Uddin & Swanpil, 2021). The results of processing satellite imagery using the NDVI method are classified as vegetation density based on (Manteri Kehutanan Republik Indonesia, 2012) which is listed in Table 3.

Based on Table 3, the NDVI varies the NDVI value -1 to -0.03 represents water or bare soil and -0.03 to 1 represents vegetation with classes. The level of NDVI value depends on density of vegetation. High NDVI values correspond to dense vegetation such as that found in tropical forest or crops at their peak growth stage.

Table 3. Vegetation index classification

No	Vegetation index	Vegetation density
1	-1- (-0.03)	No vegetation
2	-0.03-0.15	Very low
3	0.15-0.25	Low
4	0.25-0.35	Medium
5	0.35-1	high

Source: (Kementrian Perindustrian Republik Indonesia, 2021)

Furthermore, the processing results of the NDVI method are carried out by calculating the proportion of vegetation (Pv). Proportion of vegetation (vegetation fraction) is defined as the percentage of vegetation occupying the ground area in vertical projection. The proportion of vegetation Pv is closely related to NDVI values for vegetation and soil (Twumasi, et al., 2021). Pv was estimated by equation (4).

$$Pv = \left(\frac{NDVI - NDVI_{min}}{NDVI_{max} - NDVI_{min}} \right)^2 \quad (4)$$

NDVI min : minimal value of NDVI

NDVI max : maximal value of NDVI

The next step is calculating Land Surface Emissivity (LSE/ ε). LSE is a proportionally factor that scales blackbody radiance (Planck’s law) to predict emitted radiance, and it is the efficiency of transmitting thermal energy across the surface into the atmosphere (Twumasi. et al, 2021). The surface emissivity based on NDVI classes is used retrieve the final LST (Uddin & Swanpil, 2021). LST can be calculate by equation (5).

$$LST = BT / (1 + ((\lambda * BT / \rho) \ln \epsilon)) \quad (5)$$

BT : at sensor brightness temperature (°C)

λ : wavelength of emitted radiance

ε : emissivity

ρ is calculated by (6)

$$\rho = h \frac{c}{\sigma} = 1.438 \times 10^{-2} m \cdot K \quad (6)$$

Where σ is the Boltzmann constant (1.38 x 10⁻²⁵ J/K), h is Planck’s constant (6.626 x 10⁻³⁴ J s), and c is the velocity of light (2.998 x 10⁸ m/s) (Barsi, Lee, Kvaran, Markham, & Pedelty, 2014); (Azua, Nnah, & Ikwueze, 2020), (Twumasi, et al., 2021).

III. RESULTS AND DISCUSSION

Figure. 4. shows the results of NDVI analysis that have a value level of -0.611 to 0.5. The most of area Lamongan regency is medium vegetation density. Areas that have a value level -0.611 to -0.03 (no vegetation class) are areas that have high population activity (including Glagah district, Deket district, Lamongan district, Karangbinangun district, Kalitengah district, Pucuk district, Babat district, and Laren district).

Lamongan regency have undergone growth of population and economy. The changes of vegetation by asphalt and concrete for construction of roads, building, and other human activity leads to the formation of urban heat island. Rapid urban expansion and development have resulted in the conversion of many natural green surfaces within cities to non-transpiring built-up surfaces (Mensah, et al., 2020).

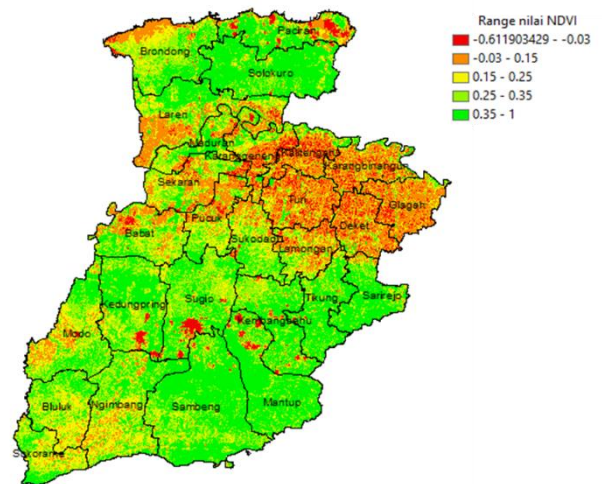


Figure. 4. NDVI Analysis of Lamongan Regency

Paciran district and Brondong district are areas bordering coast line with various ranges of NDVI values. Mantup and Sambeng districts are dominated by high vegetation density with a value range of 0.35 to 1. Field conditions in Mantup and Sambeng districts are dominated by forest land cover.

LST value is obtained by utilizing band 10 on Landsat 9 satellite imagery and extracted using the Mono-window algorithm. Figure 5. shows that the highest temperature is 29°C – 33°C around Brondong and Laren subdistrict. Lamongan Regency area is dominated by temperatures with a range of 23°C – 26°C.

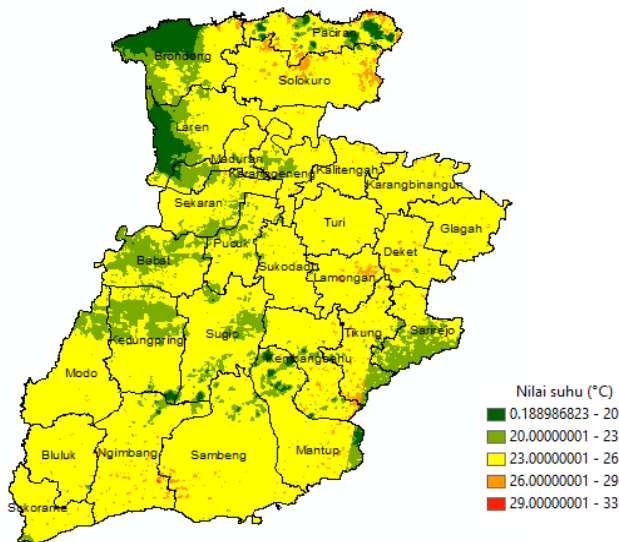


Figure. 5. NDVI Analysis of Lamongan Regency

IV. CONCLUSION

The high temperatures computed during part of the year in Lamongan regency is 29°C – 33°C. The south part of Lamongan had high vegetation cover, but the middle had less vegetation coverage. LST can be maintained by increasing vegetation land cover. The study can be informative to Lamongan Regency stakeholders on the influence of land use/ land cover on urban land surface temperature.

REFERENCES

- Azua, S., Nnah, S. I., & Ikwueze, H. U. (2020). Spatio-Temporal Variability of Land Use Land Cover and Its Impact on Land Surface Temperature in Zaria Metropolis, Nigeria. *FUTY Journal of the Environment*, 14, 1-11.
- Barsi, J. A., Lee, K., Kvaran, G., Markham, B. L., & Pedelty, J. A. (2014). The Spectral Response of the Landsat-8 Operational Land Imager. *Remote Sensing*, 6, 10232-10251. doi:<https://doi.org/10.3390/rs61010232>
- Celik, B., Kaya, S., Alganci, U., & Seker, D. Z. (2019). Assessment of the relationship between land use/cover changes and land surface temperatures: a case study of thermal remote sensing. *Fresenius Environmental Bulletin*, 28(2), 541-547. Retrieved from <https://web.csars.itu.edu.tr/assessment-of-the-relationship-between-land-use-cover-changes-and-land-surface-temperature-a-case-study-of-thermal-remote-sensing/>
- Copernicus. (2021). *Land Surface Temperature*. Retrieved from <https://land.copernicus.eu/>: [https://land.copernicus.eu/global/products/lst#:~:text=The%20Land%20Surface%20Temperature%20\(LST,direction%20of%20the%20remote%20sensor](https://land.copernicus.eu/global/products/lst#:~:text=The%20Land%20Surface%20Temperature%20(LST,direction%20of%20the%20remote%20sensor)
- Guillevic, P., Göttsche, F., Nickeson, J., Hulley, G., Ghent, D., & Yu, Y. (2018, January). Land surface temperature product validation best practice protocol version 1.1. Best Practice for Satellite Derived Land Product Validation. doi:10.5067/doc/ceoswgcv/lpv/lst.001
- Gunawan, I. (2021, March 15). Retrieved from <https://radarbojonegoro.jawapos.com/>: <https://radarbojonegoro.jawapos.com/nasional/711313031/lamongan-masuk-kawasan-percepatan-ekonomi-nasional>
- Ibrahim, M., & Mallouh, H. A. (2018). Estimate Land Surface Temperature in Relation to Land Use Types and Geological Formations Using Spectral Remote Sensing Data in Northeast Jordan. *Open Journal of Geology*, 8, 174-185. doi:<https://doi.org/10.4236/ojg.2018.82011>
- Kementrian Perindustrian Republik Indonesia. (2021, November 22). <https://kemenperin.go.id/artikel/758/Lamongan-Jadi-Sentra-Industri-Maritim>. Retrieved from <https://kemenperin.go.id/>: <https://kemenperin.go.id/artikel/758/Lamongan-Jadi-Sentra-Industri-Maritim>
- Lillesand, T. M., Kieffer, R. W., & Chipman, J. W. (2004). *Remote Sensing and Image Interpretation*. New York: Wiley.
- Manteri Kehutanan Republik Indonesia. (2012). PERATURAN MENTERI KEHUTANAN REPUBLIK INDONESIA NOMOR : P.12/Menhut-II/2012. Jakarta, DKI Jakarta, Indonesia. Retrieved from [https://jdih.menlhk.go.id/new/uploads/files/P.12%20\(5\).pdf](https://jdih.menlhk.go.id/new/uploads/files/P.12%20(5).pdf)
- Mensah, C., Atayi, J., Bah, K., Svik, M., Acheampong, D., Boateng, R. K., . . . Marek, M. V. (2020). Impact of Urban Land Cover Change on the Garden City Status and Land Surface Temperature of Kumasi. *Environmental Management and Conservation*. doi:<https://doi.org/10.1080/23311843.2020.1787738>
- Mustafa. (2020). Study for predicting Land Surface Temperature (LST) Using Landsat Data: A Comparison of Four Algorithms. *Journal Hindawi*.
- Pardede, E. D. (2010). Hubungan Suhu Permukaan dan Penutupan Lahan di wilayah Kota Medan.
- Sekertekin, A., & Bonafoni, S. (2020). Land Surface Temperature Retrieval from Landsat 5, 7, and over Rural Areas: Assessment of Different Retrieval Algorithms and Emissivity Models and

Toolbox Implementation. *Remote Sensing*, 294.
doi:<https://doi.org/10.3390/rs12020294>

- Sutariya, S., Hirapara, A., & Tiwari, M. K. (2022). Development of Modeler for Automated Mapping of Land Surface Temperature Using GIS and Landsat-8 Satellite Imagery. *International Journal of Environmental and Geoinformatics (IJECEO)*, 9(2), 54-59.
doi:<https://doi.org/10.30897/ijegeo.820906>
- Twumasi, Y. A., Merem, E. C., Namwamba, J. B., Mwakimi, O. S., Silva, T. A., Frimpong, D. B., . . . Mosby, H. J. (2021). Estimation of Land Surface Temperature from Landsat-8 OLI Thermal Infrared Satellite Data. A Comparative Analysis of Two Cities in Ghana. *Advanced in Remote Sensing*, 10, 131-149.
doi:<https://doi.org/10.4236/ars.2021.104009>
- U.S. Geological Survey. (2021). *Landsat 9*. Retrieved from landsat.gsfc.nasa.gov: landsat.gsfc.nasa.gov
- U.S. Geological Survey. (2022). Retrieved from <https://earthexplorer.usgs.gov/>: <https://earthexplorer.usgs.gov/>
- Uddin, M. J., & Swanpil, F. J. (2021). Land Surface Temperature (LST) Estimation at Kushtia District, Bangladesh. *Journal of Civil Engineering, Science and Technology*, 12(2), 214-228.
doi:<https://doi.org/10.33736/jcest.3985.2021>
- Wang, L., Lu, Y., & Yao, Y. (2019). Comparison of Three Algorithms for the Retrieval of Land Surface Temperature from Landsat 8 Images. *Sensors*.
doi:<https://doi.org/10.3390/s19225049>